Radiochimica Acta 65, 173–179 (1994)

Sorption of ^{241}Am onto Montmorillonite, Illite and Hematite Colloids

By C. Degueldre*, H. J. Ulrich and H. Silby*****

* **Paul Scherrer Institute, 5232 Villigen PSI, Switzerland**
** **formely Paul Scherrer Institute, 5232 Villigen PSI, Switzerland**
*** **Heriot-Watt University, Edinburgh, U.K.**

(Received November 16, 1993; revised March 15, 1994)

Actinide / Colloids / Sorption / Desorption / Americium / Surface complexation

Abstract

Actinide sorption on colloids may be described as a competition between the formation of complexes in solution and the build up of surface complexes. The role of particle and of carbonate concentrations on the sorption/desorption of ^{241}Am on montmorillonite, illite and hematite colloids is investigated. Since the partition coefficient (K_p) values are virtually independent of the colloid concentrations, within the range 1 to 300 ppm, no significant aggregation takes place in the sorption/desorption experiment. At pH 8, a slight decrease of K_p is observed if the concentration of total carbonate exceeds 10^{-2} M. The formation of the carbonato- (and hydroxo-carbonato-) complexes in the solution competes with the formation of surface complexes on the colloids. A relationship between the sorption coefficient and the complexation of ^{241}Am in the solution has been found. This leads to the conclusion that, besides free americium cation, the hydroxo-, and carbonato- as well as the mixed hydroxo-carbonato-complexes are sorbed. Only when the tricarbonatocomplex $[Am(CO_3)_3]^{3-}$ prevails (total carbonate concentration $>10^{-2}$ M), a significant decrease of the distribution coefficient is observed. At pH 10 this decrease disappears because under these conditions the strong hydroxo-complexes dominate. A pragmatic and relatively simple application of surface complexation model describes the observed features.

1. Introduction

The underground disposal of nuclear waste requires consideration of many processes which may affect safety. Radionuclides potentially released from nuclear waste may sorb onto colloids issuing from the engineering barriers (near-field) or onto natural colloids present in the groundwater (far-field). For strongly sorbing radionuclides, association onto colloids could have a significant influence on migration processes if the colloid concentration is sufficiently high (e.g. >1 ppm) and the colloids are mobile. Maximum transport of radionuclides by colloids occurs if sorption is irreversible and no colloid retention occurs in the hydrogeological system [1, 2].

In this study, ^{241}Am was selected as an example of a trivalent sorbing tracer. Americium distribution was determined as a function of solution parameters and the nature of the colloid. In groundwater, important parameters are the pH and the total carbonate concentration. In the hydrochemical environment, the predominant chemical reactions of the Am^{3+} ions are hydrolysis and complexation by carbonates [3, 4] when the concentration of organic ligands is low. In granitic groundwater systems, the partial pressure of CO_2 in equilibrium with the water may be different from its partial pressure in air and ranges from about 10^{-6} to 10^{-1} Atm depending on local pH (6 to 10) and alkalinity (10^{-4} to 5×10^{-3} M) [5, 6]. In the deep crystalline groundwaters, the pH is around 8 [6]. Under such conditions the complexation by carbonate may be important for Am^{3+} in that it influences its solubility, sorption on colloids and therefore its migration behaviour. Surface complexation is then the predominating sorption mechanism for Am^{3+}. Ionic interaction is important only at pH values lower [7] than those observed for the natural granitic groundwaters [6, 8].

Bentonite, which consists mainly of montmorillonite, is a potential backfilling material for a high level radioactive waste repository. The near field may be a source of colloids if local physical and chemical conditions favour colloid dispersion at the far-field interface.

On geological time scales, montmorillonite (swelling clay) can be transformed into illite (non-swelling) either by a chemical reaction in the solid state or by a dissolution/reprecipitation process [8]. It is also found as a colloidal material in granitic groundwaters [9, 10]. Illite, therefore, was also included in this study. For both clays, strongly reactive >Al–OH groups are found on the edges of the particles.

Iron oxide and hydroxide colloids may also be abundant in natural aquatic systems [11]. Iron colloids may be formed or dissolved according to Eh and/or pH changes. Sorption onto iron oxy(hydro)oxide colloids may therefore be an important factor determining the distribution of radionuclides in such systems.

2. Experimental

2.1. Colloid characterization

Sodium montmorillonite, which was used in this study, had been characterized earlier [12]. Stock colloidal solutions were obtained after a one month sedimentation. The resulting solutions were 830 ppm for mont-

* Also, Dept. of Environmental Sci., University of Geneva.
** *Present address:* Zürcher Ziegeleien, 8045 Zürich, Switzerland.

morillonite and 211 ppm for illite, with particles smaller than 1 μm.

Hematite Fe_2O_3 may be formed by dehydration of ferrihydrite obtained by rapid hydrolysis of Fe(III) solutions or by the fast oxidation of Fe(II) brought into solution. Hematite is more stable than goethite and amorphous $Fe(OH)_3$ [13]. The hematite used in this study was provided by the Swiss Federal Institute for Water Resources and Water Pollution Control and characterized by electron microscopy. The colloid size was 60−80 nm and the Fe_2O_3 concentration in the original solution was 67 $g \cdot l^{-1}$. From this suspension, a diluted stock colloidal solution (2700 ppm) was prepared in suprapure water. This stock solution was stable over several weeks and no sedimentation was required.

2.2. Radioanalytical tests

A solution of ^{241}Am was supplied by CEA (France). The activity of the stock solution (0.5 M HNO_3) was 12.8 kBq $\cdot$ ml^{-1}, corresponding to a total concentration of $4.18 \cdot 10^{-7}$ M ^{241}Am.

Americium in solution was measured by liquid scintillation using a 50% solution/50% Instagel cocktail. Calibrations showed that, over a large range of reagent concentration, no significant quenching was observed and the counting efficiency was very close to 100%.

Sorption/desorption studies were performed by batch tests (sorption) followed by desorption steps using filtration and/or dialysis. All tests, including the blanks, were run in duplicate.

2.2.1. Batch experiments

Solutions were prepared containing colloids (i.e. 100 ppm montmorillonite) and 3.6×10^{-9} M ^{241}Am. At pH 8, the solutions were buffered by 10^{-3} M tris(hydroxymethyl)-aminomethane (no effect on Am sorption), whereas, at pH 10, carbonate was used as a buffer. Total carbonate concentrations were: 10^{-4}, 10^{-3}, 10^{-2} and 0.1 M. After an equilibration phase between 1 and 10 days (preliminary tests showed that the equilibrium is reached within hours), aliquots of 20 ml were filtered through polycarbonate filters (pore size 30 nm). Activities in the filtrate and unfiltered suspension were then determined, thus allowing the calculation of the distribution coefficient K_p.

2.2.2. Dialysis tests

These tests were performed to measure sorption data without dynamic separation i.e. ultrafiltration. Losses caused by sorption to the walls of the reaction vessels and on the membranes were determined by performing blank experiments under identical conditions, without colloids.

Colloid concentrations used for the carbonate effect tests were: 83 ppm montmorillonite, 77 ppm illite and 135 ppm hematite. The pH of the 8.5×10^{-10} M ^{241}Am solution was adjusted to 8.0±0.2 by adding 10^{-2} M tris(hydroxymethyl)-aminomethane buffer. Ionic strength was maintained at 0.5 eq $\cdot$ l^{-1} by adding $NaClO_4$. Dialysis tests were performed with polyethylene test tubes (50 ml) which contained the inner solutions and which were separated by a 25 mm polycarbonate membrane (pore size 30 nm), and 100 ml polyethylene flasks containing the outer solutions. Both inner and outer solutions were thus separated by the membrane. At the start of each experiment, the inner solutions contained inert electrolyte, the buffer, $^{241}Am(III)$, and the colloids (blanks without colloids), whereas the outer solutions contained the same concentrations of inert electrolyte and buffer as the inner solutions, but without both $^{241}Am(III)$ and colloids. Dissolved ions were therefore able to diffuse through the membrane but not colloids. The systems were allowed to equilibrate for at least 5 days on a shaking machine. Distribution was determined by measuring the activities of both inner and outer solutions, respectively. Losses due to sorption on the walls were corrected by subtracting the blank effects from the samples without colloids.

A partition coefficient (K_p/ml $\cdot$ g^{-1}) was then calculated as follows:

$$K_p = \frac{[Am]_{coll}}{[Am]_l \cdot [coll]} \quad (1)$$

$[Am]_{coll}$/M is the total concentration of ^{241}Am sorbed on the colloids, $[Am]_l$/M is the total concentration of the free (not sorbed on colloid) nuclide in solution and [coll]/g $\cdot$ ml^{-1} is the concentration of the colloids.

3. Results and discussion

3.1. Effect of colloid concentration

Prior to comparing the results obtained by using the surface complexation model with the experimental data, it is useful to check if aggregation does take place [14]. In this set of experiments, the concentrations of the montmorillonite, illite and hematite colloids were varied from: 1 to 300 ppm (Fig. 1). Total carbonate was kept constant at 10^{-2} M. All other conditions were identical with those described in Section 2.2.

As can be seen from Fig. 1, a slight decrease of K_p is observed for the sorption of Am(III) when the clay concentration increases. The same effect was observed for the sorption of Cm(III) on kaolinite particles [15]. Since no strong K_p changes occurred within the range of the experimental conditions, it may be concluded that, over the experimental time period, no significant coagulation took place and that the concentration of active sorption sites was constant [14, 15]. This was also confirmed by the fact that the colloidal solutions were stable with respect to sedimentation.

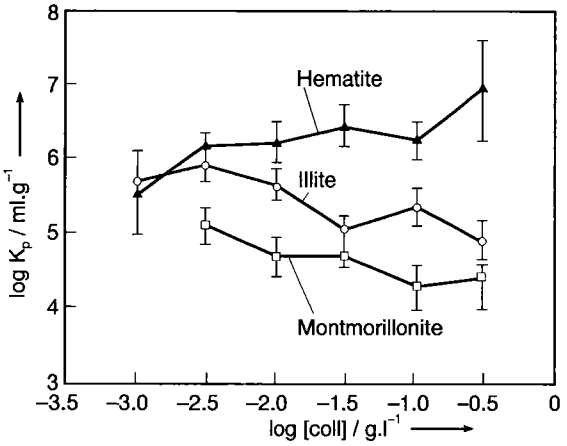

Fig. 1. Effect of the colloid concentration on K_p. *Conditions:* pH = 8, $[CO_3]_t$ = 0.01 M, [Am(III)] = 8.5×10^{-10} M, dialysis tests.

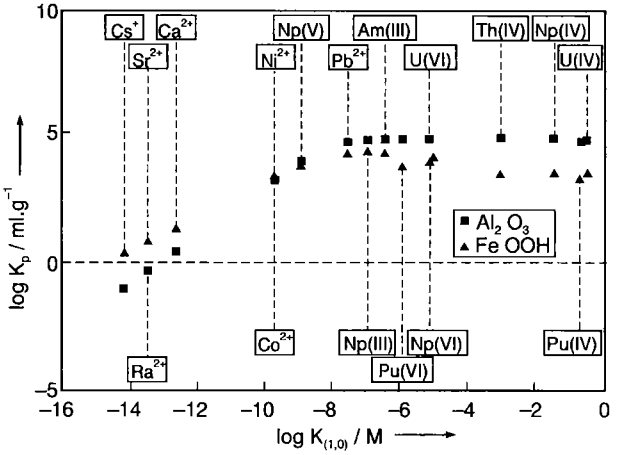

Fig. 2. K_p plot of selected species as a function of the first hydrolysis constant $K_{(1,0)}$. *Conditions:* K_p values were calculated using a non electrostatic monodentate surface complexation model, considering only hydroxo-complexes, for modeling see Section 3.2.1. (Eq. (4), and data from [22].

3.2. Modeling and experimental results

3.2.1. Hydroxo-complex formation and their sorption on colloids

For natural conditions (neutral to slightly basic pH) and for the actinides (as well as other metal ions), specific sorption is dominant, and sorption by ion exchange can be neglected for the nuclide transport by a colloid-facilitated mechanism [2, 6, 16] when the salt content in water is high enough (e.g. 10^{-2} M [7]). A non-electrostatic surface complexation model then describe the sorption.

In this Section, $K_{(i,j)}$ denotes the stepwise stability constant (and $\beta_{(i,j)}$ the stability constant) of a (i.e. i hydroxo-, j carbonato-) complex and $K_{(s,i,j)}$ the corresponding surface complexation constant. According to the model proposed by Schindler and Stumm [17], mono- and bi-dentate surface complexation constants can be correlated with the first and second hydrolysis constants $\beta_{(1,0)}$ and $\beta_{(2,0)}$ (or $K_{(1,0)}$ and $K_{(1,0)} \cdot K_{(2,0)}$) of a sorbable metal ion. For many metal ions M^{z+} showing tendency to hydrolyse, the reactions:

$$H_2O + M^{z+} \overset{K_{(1,0)}}{\rightleftharpoons} M(OH)^{(z-1)+} + H^+ \qquad \text{(in solution)}$$

and

$$>S{-}OH + M^{z+} \overset{K_{(S;0,0)}}{\rightleftharpoons} >S{-}O{-}M^{(z-1)+} + H^+ \qquad \text{(at the surface } S\text{)}$$

are analogous and the reaction thermodynamic constants may be evaluated on the basis of correlations [16].

If analogies are found between the surface complexation and the first hydrolysis reactions of mono-, bi-, tri-...valent species, and, if correlations are derived for the thermodynamic constants of these reactions, these analogies and correlations must also be applied for the mono-, di-, tri-,...hydroxo-complexes of these species with regard to their behaviour in solution and at the surface. The reaction:

$$>S{-}OH + M(OH)_i^{(z-i)+} \overset{K_{(S;i,O)}}{\rightleftharpoons} >S{-}O{-}M(OH)_i^{(z-i-1)+} + H^+ \qquad \text{(at } S\text{)}$$

might then describe the sorption of a hydrolysed species (i is limited by the coordination properties). Polynuclear hydroxo-complexes are not considered because this work deals with relatively diluted solutions. Based on data obtained for the sorption on different solid phases, sorption data of other metal elements may be predicted on the basis of the correlations between the surface complexation constants and the respective hydrolysis constants of the corresponding M^{z+} species (metal ion, hydroxo-, and later in this paper, carbonato- or mixed complexes) in solution, as illustrated in Table 1.

Table 1. Surface complexation constant $K_{(s;\,i-1,\,0)}$ correlation with the hydrolysis constant $K_{(i,0)}$
Conditions: the reference report to the original work for the $K_{(s;\,i-1,\,0)}$ determination (actually the apparent β values for pH 8 were considered), $K_{(i,0)}$ values were updated from the PSI data base [22]. The considered phases (s) are γ-Al_2O_3 and FeOOH.

Correlation	Reference
$\log K_{(Al2O3;\,i-1,\,0)} = +6.02+0.98 \log K_{(i,0)}$	[19]
$\log K_{(FeOOH;\,i-1,\,0)} = +3.75+0.75 \log K_{(i,0)}$	[20]

Herewith, the metal species distribution follows the relationship:

$$[M]_t = [M^{z+}]\,\{1 + \Sigma\,\beta_{(i,0)} \cdot [H^+]^{-i}\} \qquad (2)$$

$$[M]_{coll} = [M^{z+}]\,\{K_{(s;0,0)} + \Sigma\,K_{(s,i,0)} \cdot \beta_{(i,0)} \cdot [H^+]^{-i}\} \cdot [>SOH] \cdot [H^+]^{-1} \qquad (3)$$

where $\beta_{(i,0)}$ are the individual overall hydrolysis constants, whereas $K_{(s;0,0)}$ and $K_{(s;i,0)}$ are the surface complexation constants for the unhydrolysed metal cations and for individual hydroxo-complexes, respectively. For a given system (e.g. spherical colloids, average

Table 2. Hypothesis of analogy between soluble and surface complexes.
Hydrolysis reaction of $AmL_j^{(3-xj)+}$ species in solution e.g.

$$AmL_j^{(3-xj)+} + H_2O \Leftrightarrow AmL_j(OH)^{(2-xj)+} + H^+$$

corresponds to an analogous reaction with surface hydroxyl groups:

$$AmL_j^{(3-xj)+} + >S{-}OH \Leftrightarrow >S{-}O{-}AmL_j^{(2-xj)+} + H^+.$$

For the hydrolysable $AmL_j^{(3-xj)+}$ species, the corresponding hydrolysis products in solution and at a colloid surface are listed (j is limited by the coordination properties).

Reagent species	Product of hydrolysis	Hydrolysis constant K	Product of surface complexation	Surface complexation constant $K_{(s)}$
Am^{3+}	$Am(OH)^{2+}$	$K_{(1,0)}$	$Am{-}O{-}S<$	$K_{(s,0,0)}$
$Am(OH)^{2+}$	$Am(OH)_2^+$	$K_{(2,0)}$	$(OH){-}Am{-}O{-}S<$	$K_{(s,1,0)}$
$Am(OH)_2^+$	$Am(OH)_3$	$K_{(3,0)}$	$(HO)_2{-}Am{-}O{-}S<$	$K_{(s,2,0)}$
$Am(OH)_3$	$Am(OH)_4^-$	$K_{(4,0)}$	$(HO)_3{-}Am{-}O{-}S<$	$K_{(s,3,0)}$
$Am(CO_3)^+$	$(HO)Am(CO_3)$	$K_{(1,1)}$	$(CO_3){-}Am{-}O{-}S<$	$K_{(s,0,1)}$
$Am(CO_3)_2^-$	$(HO)Am(CO_3)_2^{2-}$	$K_{(1,2)}$	$(CO_3)_2{-}Am{-}O{-}S<$	$K_{(s,0,2)}$
$(HO)Am(CO_3)$	$(HO)_2Am(CO_3)^-$	$K_{(2,1)}$	$(HO)(CO_3){-}Am{-}O{-}S<$	$K_{(s,1,1)}$

Table 3. Am(III) hydroxo-, carbonato- and mixed complexes constants.
The logarithmic values of the cumulative formation constants for the different complexes are given as $\beta_{(i,j)}$, whereas the $K_{(i,j)}$ values are the equilibrium constants for the individual complexation reactions. The indices $_{(i)}$ and $_{(j)}$ stand for the hydroxo- and carbonato-complexes, respectively, the index i or j indicates the number of ligands, data from (4 and 21).

	log values of $\beta_{(i,j)}$ and $K_{(i,j)}$								
$\beta_{(i,j)}$ / $K_{(i,j)}$	$\beta_{(0,j)}$	$K_{(1,j)}$	$\beta_{(1,j)}$	$K_{(2,j)}$	$\beta_{(2,j)}$	$K_{(3,j)}$	$\beta_{(3,j)}$	$K_{(4,j)}$	$\beta_{(4,j)}$
$\beta_{(i,0)}$		−6.6	−6.6	−8.0	−14.6	−10.0	−24.6	−16.9	−41.5
$K_{(i,1)}$	6.5		4.3		2.0				
$\beta_{(i,1)}$	6.5	−8.8	−2.3	−10.3	−12.6				
$K_{(i,2)}$	5.3		0.8						
$\beta_{(i,2)}$	11.8	−13.3	−1.3						
$K_{(i,3)}$	1.6								
$\beta_{(i,3)}$	13.4								
$K_{(i,4)}$	−3.4								
$\beta_{(i,4)}$	10								

particle diameter 200 nm, density of reactive sites 3 per nm² [26], yielding [>SOH] in mol · l⁻¹), the distribution of some important radionuclides may be predicted by this model using the relation:

$$K_p = \frac{\{ K_{(s;0,0)} + \Sigma K_{(s;i,0)} \beta_{(i,0)} [H^+]^{-i} \} \quad [>SOH]}{\{1 + \Sigma \beta_{(i,0)} [H^+]^{-i} \} \quad [H^+] \cdot [coll]} \tag{4}$$

where [coll] is given in g of colloid per ml of solution. The K_p calculation results are reported as a function of $K_{(1,0)}$ in Fig. 2. Some elements with very weak hydrolysis constants (e.g. alkali and alkali earth metals) may also sorb much more strongly than predicted by this model because electrostatic (ion exchange) association dominates their overall sorption. The result presented in Fig. 2 for bivalent element and for actinide species is comparable to that reported by Li [18] for selected elements in sea or river water particles. It must be noted that for pH = 8, $\log K_p$ increases with $\log K_{(1,0)}$ up to pH = $-\log K_{(1,0)}$ where both M^{z+} and $M(OH)^{(z-1)+}$ are present at the same concentration (50% each). For stronger hydrolysable species, a competition starts between the built up of hydroxo-complexes in solution and surface complexes. This yields a plateau in the plot because $\log K_{(i,0)}$ is in general larger than $\log K_{(i+1,0)}$. This plateau is found at $\log K_p$ around 5 for 200 nm colloids and it would reach 6 and 7 for 20 and 2 nm colloids respectively. For seawater, the plateau found by Li [18] was around 7.

3.2.2. *Am(III) carbonato- and mixed hydroxo-carbonato-complexes formation and sorption*

For pH 8, a concentration of 10^{-4} M of carbonate [CO_3^{2-}] corresponds to a concentration of total carbonate (HCO_3^- and CO_3^{2-}) of approximately 2×10^{-2} M. The mono- and dicarbonato-complexes dominate ([4], [21]). Hydroxo-complexes make up then less than 5% of total Am(III), while at pH 8 in carbonate free solution, only hydroxo-complexes exist.

For lower total carbonate concentrations, the hydroxo-complexes become more significant. Under such conditions, the total concentration of Am (in the

liquid phase, without sorption on colloid) is given by the equation:

$$[Am^{3+}]_t = [Am^{3+}]\,(1 + \sum_{i=1}^{4}\beta_{(i,0)}\,[H^+]^{-i} + \sum_{j=1}^{4}\beta_{(0,j)}\,[CO_3]^j + \sum_{i=1,\,j=1}^{2}\beta_{(i,j)}\,[H^+]^{-i}\,[CO_3]^j) \quad (5)$$

with $\beta_{(i,0)}$ the overall constants for the hydroxo-complexes and $\beta_{(0,j)}$ the overall constants for the carbonato-complexes of Am. $\beta_{(i,j)}$'s are the constants for the formation of mixed hydroxo-carbonato-complexes.

Specific effects of the complexation on the sorption on colloids have been discussed by Erel and Morgan [23]. Preliminary model calculations (and comparison with reality) showed that, besides Am^{3+}, its hydroxo- and carbonato-complexes can also form surface complexes [25]. Furthermore, Am^{3+} forms mixed hydroxo-carbonato-complexes. In our model, all monodentate surface complexes are considered. Correlations between the first (and following) hydrolysis constants and the constants for surface complex formation (firstly metal ions, then complexes) were systematically expanded to all species which show the capability to hydrolyze. Table 2 presents the species considered as well as the hydrolysed forms and the predicted surface complexes of the relevant Am-species suggested by the correlation. Table 3 gives an overview of the constants of the hydroxo- and carbonato-complexes known and used (j is limited by coordination properties).

According to this model, all complexes (e.g. with ligand L^{x-}) which have the capability to hydrolyze also have the possibility to form surface complexes. As can be seen from Table 3, the species can undergo further hydrolysis as well as a corresponding surface complexation reaction.

$$>S{-}OH + ML_j^{(z-xj)+} \overset{K_{(S;0,j)}}{\rightleftharpoons} >S{-}O{-}ML_j^{(z-xj-1)+} + H^+ \quad (\text{at } S)$$

The $K_{(s;\,i,\,j)}$ values are then obtained by correlation using the relations given in Table 1 not only for the hydroxo- but also for carbonato- and mixed complexes.

A similar approach as this described in Section 3.2.1. is then followed to quantify the formation of the surface complexes. It yields a K_p value which may then be evaluated on the basis of Eq. (1) and using the correlations (Table 1).

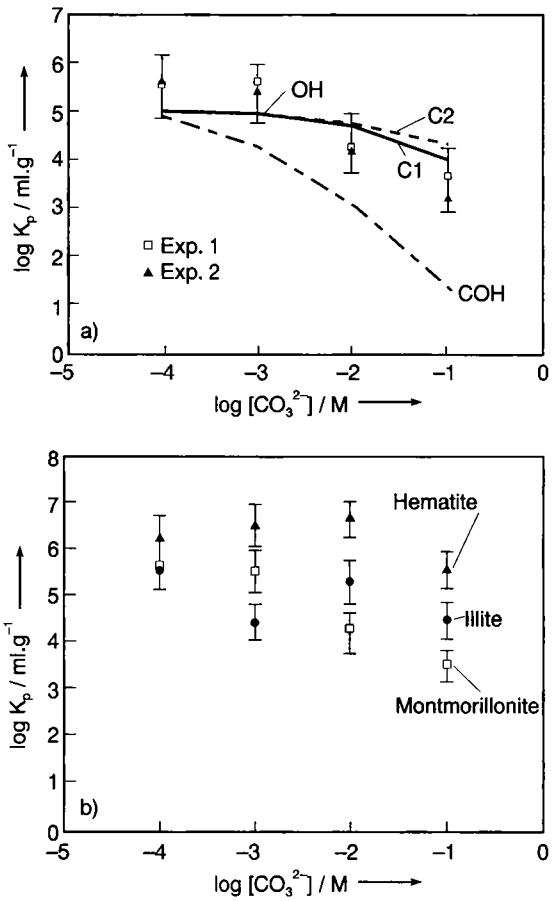

Fig. 3. Sorption at pH 8: *a:* Effect of carbonate concentration on the sorption of americium on montmorillonite (dialysis, filtration and modeling results). *b:* Effect of carbonate concentration on the sorption of americium on illite and hematite (dialysis tests). *Conditions*: experimental: dialysis [Am(III)] = 8.5×10^{-10} M, ultrafiltration [Am(III)] = 3.6×10^{-9} M, pore size 30 nm, for modeling see Section 3.2.2.; result: OH considering the sorption of hydroxo-complexes only, C1 considering sorption of hydroxo- plus monocarbonato-complexes, C2 considering hydroxo- plus mono and dicarbonato-complexes (COH same result considering potential mixed complexes).

is illustrated in Fig. 3 which shows the suggested changes of the experimental distribution coefficient K_p at pH 8 as a function of the total carbonate concentration $[CO_3^{2-}]_t$. When Am^{3+} forms carbonato-complexes in solution, the sorption behaviour is modified. The sorption is mostly influenced if the carbonate concentration exceeds 0.01 M. In order to explain the experimental behaviour, calculations were performed on the basis of the model described in Section 3.2.2. and both calculated and experimental results (filtration and dialysis) are compared for montmorillonite (Fig. 3a). For the mono-, di- and tricarbonato-complexes of ^{241}Am, distribution coefficients were calculated for the sorption of selected species (or group of

$$K_p = \frac{\{K_{(s;\,0,\,0)} + \Sigma K_{(s;\,i,\,0)}\,\beta_{(i,0)}\,[H^+]^{-i} + \Sigma K_{(s;\,0,\,j)}\,\beta_{(0,j)}\,[CO_3]^j + \Sigma v_{(s;\,i,\,j)}\,\beta_{(i,j)}\,[H^+]^{-i}\,[CO_3]^j\} \cdot [{>}SOH]}{\{1 + \Sigma\beta_{(i,0)}\,[H^+]^{-i} + \Sigma\beta_{(0,j)}\,[CO_3]^j + \Sigma\beta_{(i,j)}\,[H^+]^{-i}\,[CO_3]^j\} \cdot [H^+] \cdot [\text{coll}]} \quad (6)$$

The pragmatic and relatively simple model presented here does not account for electrostatic interactions.

3.2.3. *Effect of the carbonate concentration on the ^{241}Am sorption on the colloids*

Complexation by carbonate affects the speciation of ^{241}Am in natural systems and modifies the sorption behaviour of Am on the colloids. This postulated effect

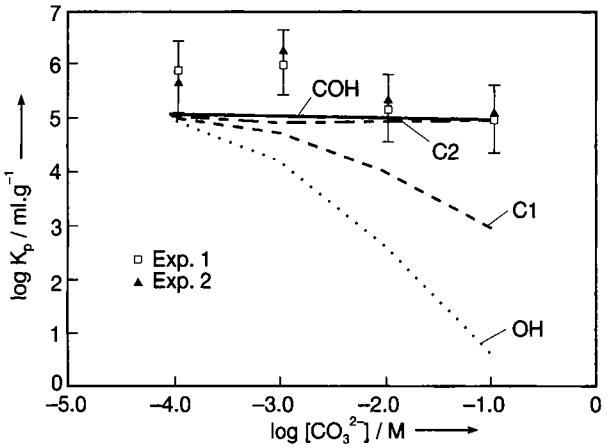

Fig. 4. Effect of the carbonate concentration on the Am(III) sorption on illite at pH 10. *Conditions*: [Am(III)] = 8.5×10^{-10} M, [illite] = 77 ppm; for modeling see Section 3.2.2.; result: OH considering the sorption of hydroxo-complexes only, C1 considering sorption of hydroxo- plus monocarbonato-complexes, C2 considering hydroxo- plus mono and di-carbonato-complexes (COH same result considering potential mixed complexes).

species) on the colloids, under uniform conditions (pH 8, ionic strength 0.5 eq $\cdot$ l^{-1}). The dependence of the K_p on the carbonate concentration is described by Eq. (6). The only adjustable parameter is the site concentration which is estimated to be equivalent of 200 nm size Al_2O_3 colloids for the clay colloids (6.25×10^{-5} mole of site $\cdot$ g^{-1} clay).

Figure 3b shows the dialysis results obtained for illite, montmorillonite and hematite. The K_p change with the carbonate concentration increase follows comparable trends. Illite results are similar to those obtained for montmorillonite which may be expected taking into account the generalization of the model described recently [26, 27]. No significant sorption behavior difference between swelling and non swelling clay was observed which confirms the suggested surface complexation mechanism.

For hematite, the build up of bidentate complexes may be considered if the site density is higher. K_p calculation on the basis of the similar model (60 nm colloid size) yielded values a bit lower than these obtained experimentally. However, estimate of site density are crucial not only for the present evaluation but also for quantification of earlier studies. In principle, the K_p for hematite and goethite should be rather similar for the same size of particle [24] and the logK_p vs. log$K$ presented in Fig. 2 should be similar, the difference coming mostly from the site density.

At pH 10, difficulties are reported because americium easily sorbs onto all vessels. Since larger corrections must be made, determination of both $[Am]_l$ and $[Am]_{coll}$ are less precise. For pH 10, no significant K_p decreases were observed when the carbonate concentration increased. However, the model presented in Section 3.2.2. is still relatively good in describing the experimental results (Fig. 4).

Acknowledgements

This work was performed at the Hot Labor, PSI, in the framework of the waste management programme. Acknowledgements are due to NAGRA, Wettingen, for the partial financial support of this study.

References

1. Smith, P., Degueldre, C.: J. Hydrol. Cont. **13**, 143–166 (1993).
2. Grauer, R.: Zur Chemie von Kolloiden: Verfügbare Sorptionsmodelle und zur Frage der Kolloidhaftung, PSI, Villigen, report No 65 (1990).
3. Cross, J., Ewart, F., Tweed, C.: Thermochemical modeling with application to nuclear waste processing and disposal. AERE, Harwell, report R 12324 (1987).
4. Robouch, P.: Contribution à la prévision du comportement de l'américium, du plutonium et du neptunium dans la géosphère; données chimiques. Rapport CEA-R-5473, France (1989).
5. Drever, J.: *The geochemistry of natural water.* Prentice-Hall, Inc., Englewood Cliffs, N. J. (1982).
6. Degueldre, C.: Colloid properties in granitic groundwater. NAGRA, Wettingen, report NTB-92-05 (1994).
7. Beall, G., Allard, B.: Trans. Am. Nucl. Soc. **32**, 164–165 (1979).
8. Grauer, R.: Bentonit als Verfüllmaterial im Endlager für hochaktiven Abfall: Chemische Aspekte, EIR, Würenlingen, Bericht Nr. 576 (1986).
9. Degueldre, C.: Grimsel Colloid Exercise: An international intercomparison exercise on the sampling and characterization of groundwater colloids, NAGRA, Wettingen, Report 90-01 (1990).
10. Pfeiffer, H.-R., Sanchez, A., Degueldre, C.: Proceedings of the 7th international symposium on water-rock interaction / Park city / Utah / USA / 13–18 July 1992, Ed. Kharaka, Y. and Maest, A. (1992), 1327–1331.
11. Miekeley, N., Countinho de Jesus, H., Porto da Silveira, C., Degueldre, C.: Chemical and physical characterization of suspended particles and colloids in waters from the Osamu Utsumi mine and Morro do Ferro analogue study, Poços de Caldas, Brazil. In: *The Poços de Caldas project: natural analogues of process in a radioactive waste repository.* Chapman, N., McKinley, I., Shea, M. and Smellie, J. Geochem. Expl. (1993), 45, No 1–3.
12. Ulrich, H.-J., Degueldre, C.: Radiochim. Acta **62**, 81–90 (1993).
13. Stumm, W., Morgan, J.: *Aquatic Chemistry.* John Wiley & Sons, New York (1981).
14. Degueldre, C., Wernli, B.: J. Environ. Radioactivity **20**, 151–167 (1993).
15. Hamilton, E.: *Application of distribution coefficients to radiological assessment models.* Eds. T. Sibley and C. Myttenaere, Elsevier Applied Science Publishers, London (1985), 35–65.
16. Schindler, P. W., Stumm, W.: *Aquatic surface chemistry,* Ed. Stumm, W., John Wiley & Sons, New York, Chichester, Brisbane, Toronto, Singapore (1987), 83–107.
17. Stumm, W., Hohl, H., Dalang, F.: Croat. Chem. Acta **48**, 491–504 (1976).
18. Li, Y.: Geochim. Cosmochim. Acta **45**, 1659–1664 (1981).
19. Hachiya, K., Sasaki, M., Saruta, Y., Mikami, N., Yasumaga, T.: J. Phys. Chem. **88**, 23–27 (1984).

20. Balistieri, L., Brewer, P., Murray, J.: Deep-Sea Res. **28A**, 101–121 (1981).
21. Kim, J.: Actinide colloid generation in groundwater. CEC report: EUR 13183 EN (1991) Commission of the European Community, Bruxelles.
22. Pearson, J., Berner, U., Hummel, W.: NAGRA Thermochemical Data Base II: supplemental data. NAGRA, Wettingen, report NTB 91-18 (1992).
23. Erel, Y., Morgan, J.: Geochim. Cosmochim. Acta **55**, 1807–1813 (1991).
24. Dzombak, D., Morel, F.: *Surface complexation modeling. Hydrous ferric oxide.* J. Wiley & Sons, New York (1990).
25. Van Cappellen, P., Charlet, L., Stumm, W., Wersin, P.: Geochim. Cosmochim. Acta **57**, 3505–3518 (1993).
26. Bradbury, M., Baeyens, B.: J. Coll. Interf. Sc. **158**, 364–371 (1993).
27. Charlet, L., Schindler, P., Spadini, L., Furrer, G., Zysset, M.: Aquat. Sci. **55**, 291–303 (1993).